JACC: CARDIOVASCULAR IMAGING VOL. 5, NO. 1, 2012

ISSN 1936-878X/$36.00

PUBLISHED BY ELSEVIER INC.

DOI:10.1016/j.jcmg.2011.05.007

Assessment of the Accuracy and Reproducibility of RV Volume Measurements by CMR in Congenital Heart Disease

Christopher J. Clarke, MD, MSc,* Matthew J. Gurka, PhD,† Patrick T. Norton, MD,‡ Christopher M. Kramer, MD,‡§ Andrew W. Hoyer, MD*‡

Charlottesville, Virginia; and Morgantown, West Virginia

OBJECTIVES The purpose of this study was to determine whether right ventricular (RV) volumes are more accurately and reproducibly measured by cardiac magnetic resonance (CMR) in an axial orientation or in a short-axis orientation in patients with congenital heart disease (CHD).

BACKGROUND There is little agreement on the most suitable imaging plane for RV volumetric analysis in the setting of abnormal RV physiology.

METHODS Measurements of RV volumes from datasets acquired in axial and short-axis orientations were made in 50 patients with CHD. RV stroke volumes (SV) calculated using these 2 methods were compared with forward flow measured in the pulmonary trunk by phase contrast (PC) imaging. Repeated volume measurements were made to assess intraobserver and interobserver reliability. Bland-Altman plots and Lin's concordance correlation coefficient (CCC) were used for all analyses of agreement.

RESULTS Analysis of all subjects revealed a statistically significant difference in interobserver reliability of RV end-systolic volume (ESV) measurements that favored the axial method ($p = 0.047$). The magnitude of measurement differences between observers in this case was small (-2.8 ml/m^2; 95% confidence interval: -5.6 to 0.0). There was no difference between the 2 contouring methods in terms of intraobserver reliability in measurements of RV end-diastolic volume (EDV), ESV, ejection fraction, or SV ($p > 0.05$ in all cases). In subjects with RV EDV $\geq$150 ml/m^2, RV SV measured using axial contours yielded better agreement with forward flow measured in the pulmonary trunk (CCC = 0.63) than did measurements made using short-axis contours (CCC = 0.56; $p = 0.007$).

CONCLUSIONS Trends favoring the axial orientation in terms of reproducibility were not clinically significant. In subjects with RV EDV $\geq$150 ml/m^2, the axial orientation yields RV volume measurements that agree more closely with flow measured in the pulmonary trunk than does the short-axis orientation. (J Am Coll Cardiol Img 2012;5:28–37) © 2012 by the American College of Cardiology Foundation

From the *Department of Pediatrics, University of Virginia Health System, Charlottesville, Virginia; ‡Department of Radiology, University of Virginia Health System, Charlottesville, Virginia; §Department of Medicine, University of Virginia Health System, Charlottesville, Virginia; and the †Department of Community Medicine, West Virginia University School of Medicine, Morgantown, West Virginia. Dr. Clarke is currently affiliated with the Department of Cardiology, Children's Hospital at Dartmouth, Manchester, New Hampshire. All authors have reported that they have no relationships relevant to the contents of this paper to disclose. Eike Nagel, MD, PhD, served as Guest Editor for this article.

Manuscript received November 3, 2010; revised manuscript received May 3, 2011, accepted May 5, 2011.

Quantification of right ventricular (RV) volumes is important for the management of patients with congenital heart disease (CHD), especially in conditions in which the RV is subject to chronic volume or pressure overload. Over time, such physiological conditions may lead to right heart failure, arrhythmia, and death. Therefore, management decisions often rely on measurements of RV size and function, and their trends during serial examinations (1–5).

Cardiac magnetic resonance (CMR) is generally considered the reference standard for quantitative assessment of right and left ventricular dimensions and function (6,7). However, because volumetric analysis requires manual contouring of the blood–myocardial boundary, the complex geometry of the RV poses certain difficulties. These difficulties are often exacerbated by abnormal RV anatomy and function, particularly at the tricuspid and pulmonary valve planes and along the ventricle's diaphragmatic surface.

CMR offers highly reproducible RV volume measurements (8,9). Several studies have compared the interobserver and intraobserver reliability of axial versus short-axis contouring methods, and the results suggest that the axial orientation is superior for normal hearts and for those with a dilated RV (10,11). However, the clinical significance of these differences in reproducibility has been unconvincing to most practitioners of CMR, given that new work has continued to use the short-axis orientation for RV volume quantification (9,12,13–15).

In addition, uncertainty exists as to the most accurate method of RV volume quantification. Conclusions regarding accuracy cannot be drawn from analyses of reproducibility. Furthermore, there is no method to reliably measure the true volume of the RV in vivo, beyond the capabilities of CMR, to serve as a basis for comparison. However, CMR does offer an additional independent method of determining RV stroke volume (SV), free from the limitations of endocardial contour tracing: quantitative flow measurement within the pulmonary trunk by phase contrast (PC) imaging (14,16,17). Thus, the question of accuracy can be addressed by examining which contour tracing method yields an RV SV that best agrees with that obtained by PC imaging.

The aim of this study was to determine whether RV volumes are more accurately and reproducibly measured by CMR in an axial orientation or in a short-axis orientation in patients with CHD.

METHODS

Subjects. CMR studies of patients with CHD and associated RV pathology, referred for CMR between January 2006 and December 2009, were reviewed. Subjects were identified retrospectively by searching the radiology database at our institution. Inclusion criteria consisted of CHD with an associated pressure and/or volume load on the RV, complete acquisition of both axial and short-axis datasets, and PC imaging acquired in a cross-sectional plane within the pulmonary trunk. Subjects with ventricular level shunts and more than mild tricuspid insufficiency were excluded.

Cardiac magnetic resonance. CMR studies were performed using 1 of 2 commercially available 1.5-T scanners (MAGNETOM Avanto and MAGNETOM Sonata, Siemens Healthcare, Erlangen, Germany). Imaging was performed with subjects in the supine position. To optimize signal-to-noise ratio, infants were imaged using the smallest coil (head or knee) that accommodated the patient's shoulder width. A 6-element radiofrequency spine array with either a dual- or 24-element body coil (depending on the scanner) was used to image larger patients. For younger subjects unable to cooperate with breath holding, imaging was performed under general anesthesia with multiple averages. Ventricular dimensions were assessed using an electrocardiographic-gated, steady-state free precession imaging sequence. Imaging parameters were tailored to patient size and heart rate to optimize spatial and temporal resolution (repetition time = 13.9 to 38.2 ms, echo time = 1.1 to 1.9 ms, field of view = 138 to 360 × 180 to 390 mm, matrix size = 108 to 192 × 144 to 192, slice thickness = 4 to 8 mm, interslice gap = 0% to 20%, reconstructed images per cardiac cycle = 25 to 38, and number of signal averages = 1 to 5). Cine images were acquired in stacked axial and short-axis datasets. For the axial dataset, localizing images were used to plan a stack of slices that covered the heart from a level just above the diaphragm to above the pulmonary bifurcation. For the short-axis dataset, the left ventricle long-axis and 4-chamber cine images were used to plan a stack of slices, parallel to the mitral valve annulus, that covered both ventricles in their entirety. Retrospective gating was used for all steady-state free precession imaging. For a given subject, axial and short-axis cine images had the same number of reconstructed phases.

ABBREVIATIONS AND ACRONYMS

CCC = concordance correlation coefficient
CHD = congenital heart disease
CI = confidence interval
CMR = cardiac magnetic resonance
EDV = end-diastolic volume
EF = ejection fraction
ESV = end-systolic volume
PC = phase contrast
RV = right ventricle
RV-PA = right ventricle to pulmonary artery
SV = stroke volume

JACC: CARDIOVASCULAR IMAGING, VOL. 5, NO. 1, 2012
JANUARY 2012:28–37

Flow measurements were performed in a cross-sectional plane within the proximal pulmonary trunk using a velocity-encoded PC imaging sequence (repetition time = 8.1 to 22.9 ms, echo time = 2.4 to 4.7 ms, field of view = 150 to 360 × 200 to 420 mm, matrix size = 88 to 256 × 144 to 300, slice thickness = 4 to 8 mm, velocity-encoding = 150 to 480 cm/s, reconstructed images per cardiac cycle = 15 to 30, and number of signal averages = 1 to 3). Images were acquired during periods of breath holding, or with signal averaging for those subjects unable to cooperate with breath-hold instructions. Retrospective gating was used predominantly for PC imaging.

CMR data were analyzed using commercially available software (Argus, Siemens Healthcare). Contour tracing was performed manually after review of cine images in movie mode. In both the axial and short-axis datasets, the first phase of each cine image was defined as end diastole. The phase of end systole was defined visually by the observer as the phase with the smallest RV volume. Contours were drawn at the boundary between the blood pool and the compact myocardium (Fig. 1). Trabeculations and papillary muscles were included as part of the RV volume. In axial datasets, contours were drawn up to the tricuspid valve and closed by a straight line across the tricuspid valve annulus. At the uppermost slices, the area below the level of pulmonary valve tissue was included in the RV volume. Identification of pulmonary valve tissue was facilitated by the simultaneous display of a cross-referenced cine image aligned longitudinally with the RV outflow tract.

In short-axis datasets, only the area of the RV outflow tract below the level of visible pulmonary valve tissue was included in the RV volume. At the inflow portion of the RV, only the area of the blood pool surrounded by trabeculated ventricular myocardium was included in the RV volume. Identification of the tricuspid valve annulus was facilitated by the simultaneous display of a cross-referenced 4-chamber cine image. The workstation calculated end-systolic and end-diastolic RV volumes using the method of summation of discs. The RV SV was calculated by subtracting the end-systolic volume (ESV) from the end-diastolic volume (EDV). The RV ejection fraction (EF) was calculated by dividing the SV by the EDV.

To quantify flow within the proximal pulmonary trunk by PC imaging, a region of interest was drawn manually around the vessel lumen in each phase of the dataset using the gradient echo image; contours were then correlated with the corresponding phase image. The workstation calculated flow volumes within the pulmonary trunk by integrating the instantaneous velocity within the region of interest over the cardiac cycle as previously de-

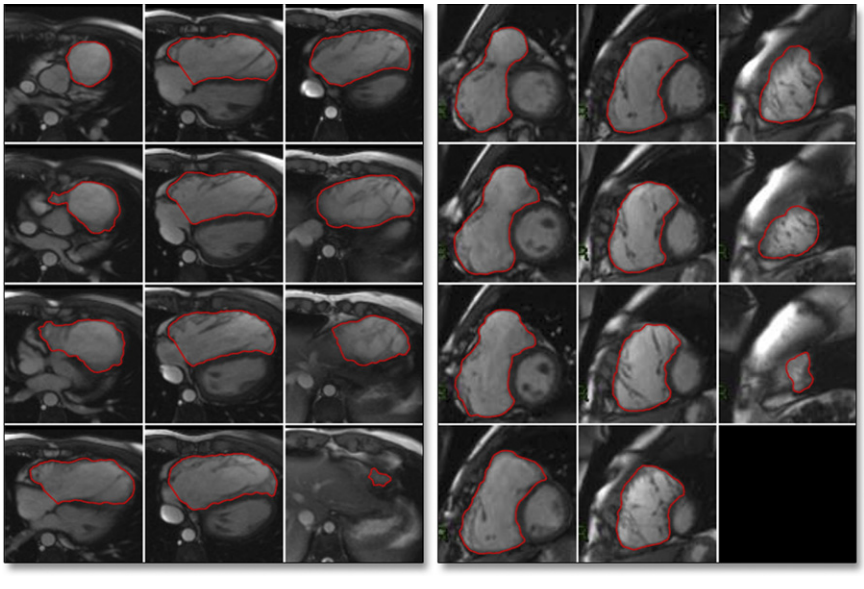

Figure 1. Sample Images of Endocardial Contours

Sample images of manually traced endocardial contours **(red lines)** of the right ventricle in end-diastole from a 15-year-old patient with tetralogy of Fallot who underwent corrective surgery as an infant (patch closure of ventricular septal defect and transannular patch augmentation of the right ventricular outflow tract). **Left:** axial slices; **right:** short-axis slices.

scribed (17). The total RV SV, as measured by PC imaging, was considered to be equal to the total forward volume of flow within the pulmonary trunk, as this reflects the total volume ejected from the RV during systole. All volumes measured by both contour tracing and PC imaging were indexed by dividing the absolute volume by the subject's body surface area.

Because flow measurements made using PC imaging may be subject to error caused by complex flow patterns or local eddy currents within the vessel of interest (18–21), the first observer (C.J.C.) performed a baseline flow correction using a background region of interest in stationary tissue as close to the position of the main pulmonary trunk in the phase encoding direction as possible. A subanalysis using these baseline-corrected values was performed to determine whether such background-phase offset errors affected the results.

To determine interobserver and intraobserver reliability, all datasets were measured 3 times. Each measurement required the selection of slices, the definition of end systole, the tracing of endocardial contours, and the drawing of the region of interest within the pulmonary trunk. Two observers measured the datasets independently and were unaware of the results of the other measurements. All measurements were made once by the first observer and twice by the second observer (A.W.H.). A period of at least 1 week elapsed between the 2 measurements made by the second observer. The first observer was a pediatric cardiology fellow with 2 years of experience in CMR of patients with CHD. The second observer was a pediatric cardiologist with advanced training in CMR of patients with CHD and 4 years of CMR experience.

Statistical analysis. Mean values and standard deviations among patients were calculated for all measurements. Median values and ranges were calculated for discrete variables. Lin's concordance correlation coefficient (CCC) was used to assess agreement of RV SV as calculated from each of the 2 contour tracing methods, with RV SV as measured by PC imaging (22). A CCC value of 1 indicates perfect agreement; values <0.5 were considered to be poor agreement, values between 0.5 and 0.7 to be moderate agreement, and values >0.7 to be good to excellent agreement. In all instances, the mean values of the multiple measurements obtained on each CMR (1 from the first investigator and 2 from the second investigator) were used to measure the agreement statistics of interest. Agreement was also assessed using the method of Bland and Altman (23). A paired sample *t* test was used to compare the resulting differences in measurements between the 2 methods. Intraobserver and interobserver reliability was also assessed using Lin CCC and the Bland-Altman method. In the analysis of intraobserver reliability, the 2 measurements made by the second observer were compared with each other. In the analysis of interobserver reliability, the first of the 2 measurements made on each CMR by the second investigator were compared to those made by the first. A Wilcoxon rank sum test was used to compare discrete variables.

A paired equivalence test, as described by Schuirmann (24), served as the basis for an a priori power analysis. With respect to the mean difference between measurements of RV SV, a 95% confidence interval (CI) half-width of 5 ml/m^2 was considered to be clinically significant. At the 0.05 level, assuming a constant standard deviation of 16 ml/m^2 on the basis of pilot data from this sample, it was determined that 49 subjects were needed to achieve a power of 0.80. An absolute difference of 10 ml/m^2 was considered to be clinically significant and a p value <0.05 was considered statistically significant.

RESULTS

Fifty patients met the criteria for inclusion in this study. Demographic data and subjects' cardiac anatomy at the time of CMR are summarized in Table 1. A median of 14 slices (range 9 to 22) were selected for the axial datasets, and a median of 12 slices (range 8 to 22) were selected for the short-axis datasets. The median number of slices selected for each dataset was the same for both investigators. Slices comprising axial datasets (6 mm, range 4 to 8) were thinner than those comprising short-axis datasets (7 mm, range 5 to 8; $p < 0.0001$), and the matrix was finer for the axial datasets (pixel size 2.3 ± 0.9 mm^2) than for the short-axis datasets (pixel size 2.5 ± 0.9 mm^2; $p = 0.006$). There was no difference in the average R-to-R interval between axial and short-axis datasets (793 ± 188 ms and 805 ± 212 ms, respectively; $p = 0.977$).

Table 2 lists the mean ± SD values for the volume measurements and EF made using each of the 2 contour tracing methods and the RV SV as measured by PC imaging. Table 2 also shows CCCs and mean bias values measuring agreement of each of the 2 contouring methods with the PC measure of RV SV. Scatterplots of these data are shown in Figure 2. With respect to RV SV as

JACC: CARDIOVASCULAR IMAGING, VOL. 5, NO. 1, 2012
JANUARY 2012:28–37

Table 1. Demographic Data

	All Patients (N = 50)
Age, yrs	17.0 ± 11.2
Male gender	29 (58)
Body surface area, m^2	1.5 ± 0.5
Congenital heart disease	
Tetralogy of Fallot, corrected	29
Transvalvar patch	15
RV-PA conduit	12
Infundibular patch and valvotomy	2
Pulmonary stenosis, valvar	6
Valvotomy	3
Transvalvar patch	1
Balloon valvuloplasty	1
No intervention	1
Partial anomalous pulmonary venous return	6
Isolated	3
Associated atrial septal defect	3
d-Transposition of the great arteries, corrected	4
Arterial switch operation, resultant pulmonary stenosis	3
Rastelli operation	1
Truncus arteriosus, corrected	3
RV-PA conduit	2
RV-PA conduit and residual atrial septal defect	1
Atrial septal defect, isolated	1
Double outlet right ventricle, RV-PA conduit	1

Values are n, n (%), or mean ± SD.
RV-PA = right ventricle-to-pulmonary artery.

measured by PC imaging, the 2 contouring methods demonstrated good agreement. The mean bias of the short-axis measure of RV SV was statistically significant (p = 0.047). However, the 95% CI of the mean bias (−7.0 to −0.1 ml/m^2) did not include values of a difference considered to be clinically meaningful. Additionally, the difference of mean biases between the 2 methods (short-axis vs. axial) did not reach statistical (p = 0.127) significance.

Analysis using baseline flow–corrected PC measurements of RV SV (first observer data only) did reveal a statistical difference in agreement between PC imaging and the 2 contouring methods, which favored the axial orientation (p = 0.007). However, the mean bias of each of the contouring methods was small (axial: −1.0 ml/m^2; 95% CI: −4.0 to 2.0 and short-axis: 2.0 ml/m^2; 95% CI: −1.1 to 5.1), as was the difference of mean biases between the 2 methods (−3.0 ml/m^2; 95% CI: −5.2 to −0.9).

A subanalysis on subjects with the largest RV volumes (EDV ≥150 ml/m^2 as measured by either observer) was performed (n = 21). These results are shown in Table 3. In this group, there was moderate agreement between RV SV as measured by PC imaging and each of the contouring methods. The difference of mean biases between the 2 methods (short-axis vs. axial) was statistically significant (p = 0.007) and favored the axial method. In addition, the 95% CI of the short-axis mean bias included differences considered to be clinically significant (−0.1 to 14.3 ml/m^2), and that of the axial method did not (−4.1 to 9.4 ml/m^2).

The intraobserver reliability of RV EDV, ESV, and SV measurements was excellent for both contouring methods (Table 4). In each case, both methods yielded similar CCCs and small mean differences (p > 0.05 for all measurements). The same was true in the subanalysis performed on subjects with RV EDV ≥150 ml/m^2 (p > 0.05 for all measurements). Scatterplots of intraobserver reliability are shown in Figure 3.

The interobserver reliability of each volume measurement was good for both methods (Table 5). A mean difference among EDV measurements of −9.2 ml/m^2 and −9.5 ml/m^2 (axial and short-axis, respectively) and among ESV measurements of −9.8 ml/m^2 and −12.7 ml/m^2 (axial and short-axis, respectively) was observed. The degree of this difference was the same for axial and short-axis measurements of EDV (p = 0.853). The difference in

Table 2. Volumetric Data and Axial Versus Short-Axis Agreement With PC Imaging

N = 50	PC Imaging	Axial Contours	Short-Axis Contours	Difference of Mean Biases
RV EDV, ml/m^2		140 ± 47	137 ± 45	
RV ESD, ml/m^2		81 ± 32	80 ± 31	
RV EF, %		43 ± 8	45 ± 7	
RV SV, ml/m^2	61 ± 22	59 ± 19*	58 ± 18†	
CCC		0.84 (0.75 to 0.90)	0.81 (0.70 to 0.88)	
Mean bias, ml/m^2		−2.1 (−5.4 to 1.2)	−3.5 (−7.0 to −0.1)	1.4 (−0.4 to 3.2) p = 0.127

Values are mean ± SD or mean (95% CI). *p = 0.204 compared with RV SV by PC imaging; †p = 0.047 compared with RV SV by PC imaging.
CCC = concordance correlation coefficient; CI = confidence interval; EDV = end-diastolic volume; EF = ejection fraction; ESV = end-systolic volume; PC = phase contrast; RV = right ventricle; SV = stroke volume.

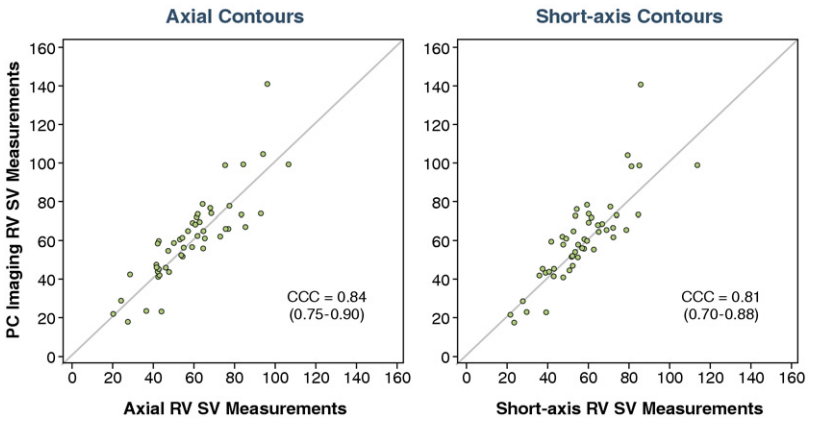

Figure 2. Scatterplots of RV SV as Measured by PC Imaging Versus Contour Tracing

Scatterplots of right ventricular (RV) stroke volume (SV) as measured by phase contrast (PC) imaging versus RV SV as measured by axial contour tracing (left) and short-axis contour tracing (right), shown with 45° lines of concordance and concordance correlation coefficient (CCC) (95% confidence interval [CI]). Measurements expressed in milliliters per square meter.

interobserver reliability between axial and short-axis measurements of ESV was statistically significant ($p = 0.047$). In this case, the absolute difference of mean differences between observers was small (-2.8 ml/m^2; 95% CI: -5.6 to 0.0). There was no significant difference between the 2 contouring methods in terms of interobserver reliability in subjects with RV EDV ≥150 ml/m^2 ($p > 0.05$ for all measurements). Scatterplots of interobserver reliability are shown in Figure 4.

DISCUSSION

In this analysis of RV volume quantification, when all subjects were analyzed, statistical trends that favored the use of the axial dataset in terms of accuracy did not represent a clinically meaningful difference between the 2 imaging orientations. However, in those patients with the largest RV (EDV ≥150 ml/m^2), the axial orientation yielded RV volume measurements that agreed more closely with flow measured in the pulmonary trunk. One explanation for this may be that as the RV dilates, the cross-sectional area of its base becomes enlarged relative to the size of the RV cavity. Because through-plane motion of the tricuspid valve annulus occurs at this location in short-axis datasets, difficulty in identifying the basal boundary of the RV using the short-axis method may result in greater error compared with the axial method. This may be an important finding because patients with substantial RV enlargement often undergo CMR examination to determine appropriate timing of interventions to reduce RV volume overload.

Analysis of intraobserver reliability revealed slightly narrower limits of agreement and slightly greater absolute CCC values for all measurements made in the axial orientation. However, this trend toward superior intraobserver reliability using the axial orientation did not reach statistical significance. In the analysis of interobserver reliability, differences between axial and short-axis measurements of ESV did reach sta-

Table 3. Volumetric Data and Axial Versus Short-Axis Agreement With PC Imaging in Subjects With RV EDV ≥150 ml/m^2

N = 21	PC Imaging	Axial Contours	Short-Axis Contours	Difference of Mean Biases
RV EDV, ml/m^2		185 ± 29	180 ± 30	
RV ESD, ml/m^2		110 ± 24	109 ± 22	
RV EF, %		41 ± 6	41 ± 6	
RV SV, ml/m^2	78 ± 20	75 ± 14*	71 ± 15†	
CCC		0.63 (0.33 to 0.81)	0.56 (0.23 to 0.77)	
Mean bias, ml/m^2		2.6 (−4.1 to 9.4)	7.1 (−0.1 to 14.3)	−4.5 (−7.6 to −1.4) p = 0.007

Values are mean ± SD or mean (95% CI). *p = 0.424 compared with RV SV by PC imaging; †p = 0.052 compared with RV SV by PC imaging.
Abbreviations as in Table 2.

Table 4. Intraobserver Reliability of Axial and Short-Axis Contour Tracing Methods

N = 50	Axial Contours	Short-Axis Contours	Difference of Mean Differences
RV EDV			
CCC	0.99 (0.98 to 1.00)	0.99 (0.98 to 0.99)	
Mean difference, ml/m^2	3.4 (1.9 to 4.9)	1.5 (−0.4 to 3.4)	−1.9 (−4.4 to 0.5) p = 0.123
RV ESV			
CCC	0.98 (0.97 to 0.99)	0.98 (0.96 to 0.99)	
Mean difference, ml/m^2	3.7 (2.3 to 5.1)	1.6 (−0.2 to 3.5)	−2.1 (−4.2 to 0.1) p = 0.057
RV EF			
CCC	0.91 (0.85 to 0.95)	0.82 (0.70 to 0.89)	
Mean difference, %	−1 (−2 to 0)	−1 (−2 to 1)	0 (−2 to 1) p = 0.553
RV SV			
CCC	0.96 (0.94 to 0.98)	0.94 (0.90 to 0.97)	
Mean difference, ml/m^2	−0.3 (−1.8 to 1.2)	−0.1 (−1.9 to 1.6)	0.1 (−2.2 to 2.4) p = 0.917

Values are mean (95% CI).
Abbreviations as in Table 2.

tistical significance, which favored the axial orientation. However, the magnitude of measurement differences between observers in this case was small and likely does not represent a clinically meaningful difference in interobserver reliability. One possible explanation for the trends favoring

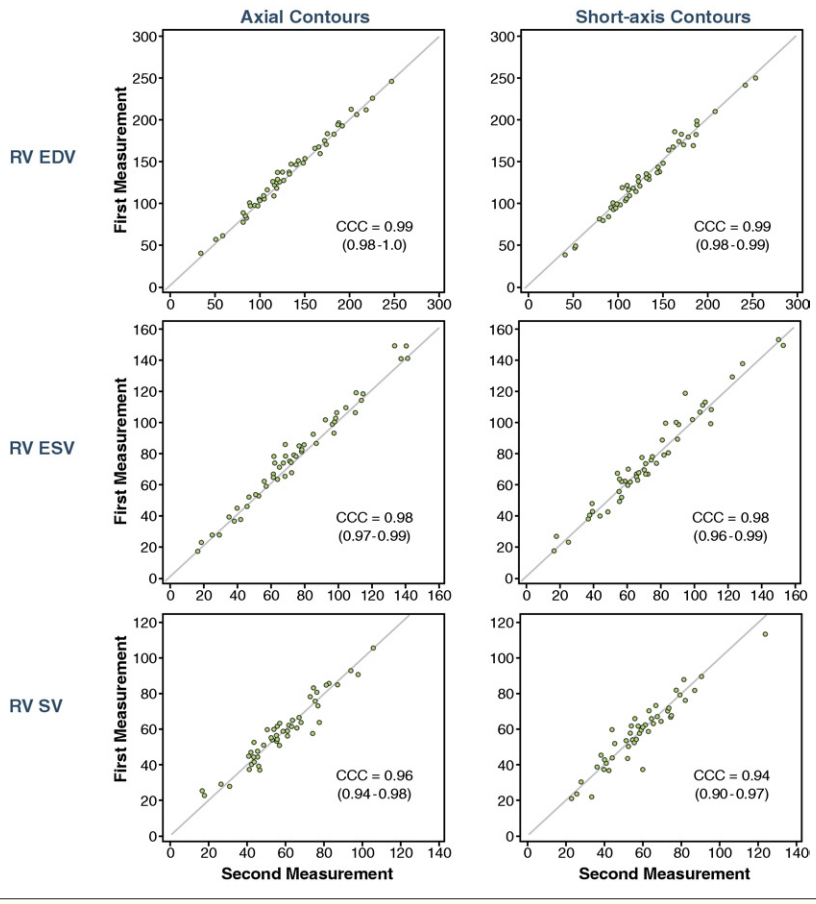

Figure 3. Scatterplots of Single Observer's First Versus Second RV Volume Measurements

Scatterplots of a single observer's first RV volume measurements versus second RV volume measurements by axial contour tracing **(left)** and short-axis contour tracing **(right)**, shown with 45° lines of concordance and CCC (95% CI). Measurements expressed in milliliters per square meter. EDV = end-diastolic volume; ESV = end-systolic volume; other abbreviations as in Figure 2.

Table 5. Interobserver Reliability of Axial and Short-Axis Contour Tracing Methods

N = 50	Axial Contours	Short-Axis Contours	Difference of Mean Differences
RV EDV			
CCC	0.97 (0.95 to 0.98)	0.95 (0.91 to 0.97)	
Mean difference, ml/m^2	−9.2 (−11.1 to −7.3)	−9.5 (−12.8 to −6.2)	−0.3 (−3.6 to 3.0) p = 0.853
RV ESV			
CCC	0.93 (0.90 to 0.96)	0.88 (0.81 to 0.92)	
Mean difference, ml/m^2	−9.8 (−11.9 to −7.8)	−12.7 (−15.7 to −9.6)	−2.8 (−5.6 to 0.0) p = 0.047
RV EF			
CCC (95% CI)	0.79 (0.68 to 0.87)	0.62 (0.47 to 0.74)	
Mean difference, %	4 (2 to 5)	5 (4 to 7)	−2 (−3 to 0) p = 0.063
RV SV			
CCC	0.96 (0.94 to 0.98)	0.91 (0.86 to 0.95)	
Mean difference, ml/m^2	0.7 (−0.8 to 2.1)	3.2 (1.2 to 5.1)	2.5 (−0.1 to 5.1) p = 0.060

Values are mean (95% CI).
Abbreviations as in Table 2.

the axial orientation is that thinner slices and finer matrices among axial datasets provided better definition of the endomyocardial border.

The differences in measurements of EDV and ESV between observers indicate that there was a systematic difference in contouring among the 2

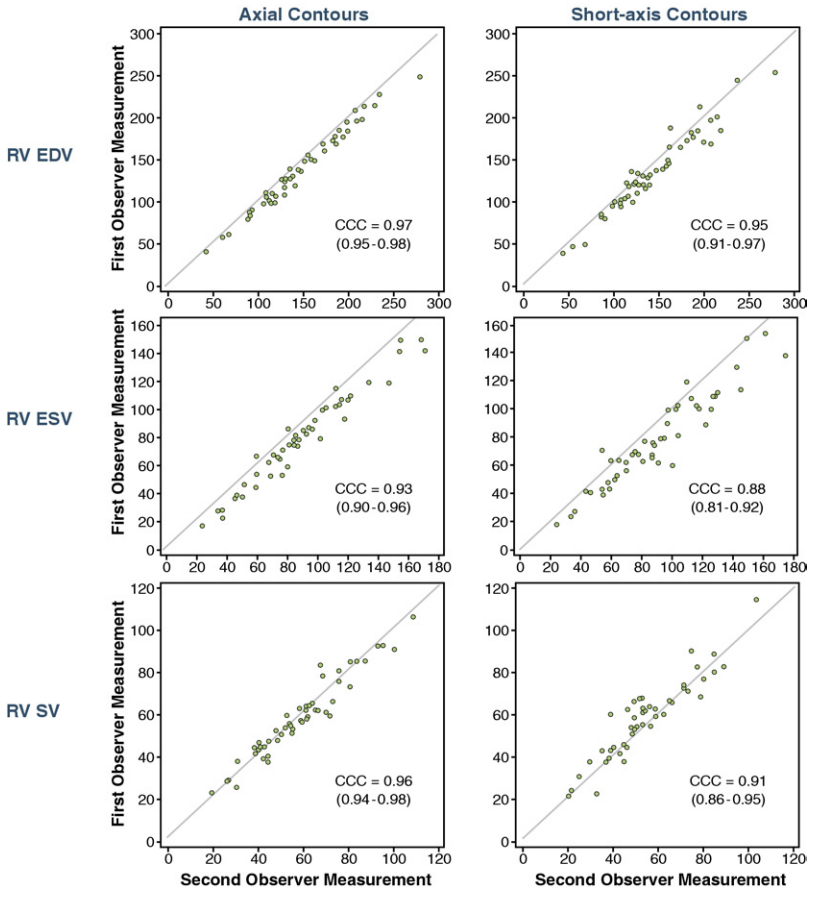

Figure 4. Scatterplots of First Observer Versus Second Observer RV Volume Measurements

Scatter plots of first observer's RV volume measurements versus second observer's RV volume measurements by axial contour tracing **(left)** and short-axis contour tracing **(right)**, shown with 45° lines of concordance and CCC (95% CI). Measurements expressed in milliliters per square meter. Abbreviations as in Figures 2 and 3.

observers. As the median number of slices selected for each dataset was the same for both observers, this likely represents a consistent difference in defining the boundary between the blood pool and the compact myocardium. This finding highlights the need for ongoing assessment of interobserver reliability in clinical practice.

There are potential limitations of this study. First, flow measurements made using PC imaging may be subject to error caused by complex flow patterns or local eddy currents within the pulmonary trunk, which may limit the ability of PC data to serve as a reference standard (18–21). However, results from an analysis using stationary tissue to baseline-correct flow measurements did not differ from results using non–baseline-corrected data in a clinically meaningful way. Recent studies have shown that use of a stationary phantom technique to perform baseline correction of flow measurements is possible in patients with CHD (18,21) and may offer advantages over the use of stationary tissue (19). Additionally, an assessment of agreement between net forward flow measured in both great arteries (excluding those subjects with shunt lesions) would have provided a check for internal consistency in flow measurements. Unfortunately, the retrospective design of this study precluded such an analysis. Although flow mapping may be subject to error under some circumstances, it offers an appropriate measure by which to compare the accuracy of contour tracing techniques in the absence of a method to measure in vivo the true volume of the RV. A second limitation is the retrospective nature of the data collection, which precluded the implementation of a uniform imaging protocol for all patients. Third, the subjects were heterogeneous (e.g., pre- and post-operative, differing forms of CHD). However, all subjects had RV pathology and represent a common group of patients referred for CMR. Fourth, the subanalysis on subjects with RV EDV $\geq$150 ml/m^2 may have been underpowered to detect a significant difference in intraobserver and interobserver reliability. Last, it is possible that a consistent bias in EDV and ESV contours could yield a SV internally consistent with PC measurements, without reflecting the true RV volumes. However, consistency between measurements of SV made using CMR does speak to the accuracy of these measurements and offers a feasible way to assess the accuracy of RV contouring.

This is the first study to analyze both reproducibility and accuracy of RV volume quantification in patients with CHD. Sarikouch et al. (14) recently reported a high degree of agreement between axial, short-axis, and phase contrast data in normal patients, and Fratz et al. (11) evaluated the reproducibility of the axial versus short-axis method in patients with tetralogy of Fallot. The results of the present study are important because CMR has become the technique of choice for assessing RV size and function in patients with CHD, and although general guidelines for CMR imaging of patients with CHD have been developed (25–27), definitive recommendations for a standardized approach to RV volumetric analysis are lacking. The results of this study may help guide the development of such recommendations in the future.

Reprint requests and correspondence: Dr. Christopher J. Clarke, Children's Hospital at Dartmouth, Dartmouth-Hitchcock Clinic, 100 Hitchcock Way, Manchester, New Hampshire 03104. *E-mail: Christopher.J.Clarke@Hitchcock.org.*

REFERENCES

1. Geva T. Indications and timing of pulmonary valve replacement after tetralogy of Fallot repair. Semin Thorac Cardiovasc Surg Pediatr Card Surg Ann 2006;9:11–22.
2. Oosterhof T, Van Straten A, Vilegen HW, et al. Preoperative thresholds for pulmonary valve replacement in patients with corrected tetralogy of Fallot using cardiovascular magnetic resonance. Circulation 2007;116:545–51.
3. Knauth AL, Gauvreau K, Powell AJ, et al. Ventricular size and function assessed by cardiac MRI predicts major adverse clinical outcomes late after tetralogy of Fallot repair. Heart 2008; 94:211–6.
4. Lorenz CH, Walker ES, Graham TP Jr., Powers TA. Right ventricular performance and mass by use of Cine MRI late after atrial repair of transposition of the great arteries. Circulation 1995;92 Suppl 9:II233–9.
5. Davlouros PA, Kilner PJ, Hornung TS, et al. Right ventricular function in adults with repaired tetralogy of Fallot assessed with cardiovascular magnetic resonance imaging: detrimental role of right ventricular outflow aneurysms or akinesia and adverse right-to-left ventricular interaction. J Am Coll Cardiol 2002;40:2044–52.
6. Maceira AM, Prasad SK, Khan M, Pennell DJ. Reference right ventricular systolic and diastolic function normalized to age, gender, and body surface area from steady-state free precession cardiovascular magnetic resonance. Eur Heart J 2006;27:2879–88.
7. Keenan NG, Pennell DJ. CMR of ventricular function. Echocardiography 2007;24:185–93.
8. Grothues F, Moon JC, Bellenger NG, Smith GS, Klein HU, Pennell DJ. Interstudy reproducibility of right ventricular volumes, function, and mass with cardiovascular magnetic resonance. Am Heart J 2004;147:218–23.
9. Mooij CF, de Witt CJ, Graham DA, Powell AJ, Geva T. Reproducibility of MRI measurements of right ventricular size and function in patients with normal and dilated ventricles. J Magn Reson Imaging 2008;28:67–73.

10. Alfakih K, Plein S, Bloomer T, Jones T, Ridgeway J, Sivananthan M. Comparison of right ventricular volume measurements between axial and short axis orientation using steady-state free precession magnetic resonance imaging. J Magn Reson Imaging 2003;18:25–32.
11. Fratz S, Schuhbaeck A, Buchner C, et al. Comparison of accuracy of axial slices versus short-axis slices for measuring ventricular volumes by cardiac magnetic resonance in patients with corrected tetralogy of Fallot. Am J Cardiol 2009;103:1764–9.
12. Luijnenburg SE, Robbers-Visser D, Moelker A, Vliegen HW, Mulder BJM, Helbing WA. Intra-observer and interobserver variability of biventricular function, volumes and mass in patients with congenital heart disease measured by CMR imaging. Int J Cardiovasc Imaging 2010;26:57–64.
13. Buechel EV, Kaiser T, Jackson C, Schmitz A, Kellenberger CJ. Normal right- and left ventricular volumes and myocardial mass in children measured by steady state free precession cardiovascular magnetic resonance. J Cardiovasc Magn Reson 2009;11:19.
14. Sarikouch S, Peters B, Gutberlet, et al. Sex-specific pediatric percentiles for ventricular size and mass as reference values for cardiac MRI. Circ Cardiovasc Imaging 2010;3:65–76.
15. Samyn MM, Powell AJ, Garg R, Sena L, Geva T. Range of ventricular dimensions and function by steady-state free precession cine MRI in repaired tetralogy of Fallot: right ventricular outflow tract patch vs. conduit repair. J Cardiovasc Magn Reson 2007;26:934–40.
16. Jeltsch M, Ranft S, Klass O, Achoff AJ, Hoffman MHK. Evaluation of accordance on magnetic resonance volumetric and flow measurements in determining ventricular stroke volume in cardiac patients. Acta Radiol 2008;49:530–9.
17. Powell AJ, Maier SE, Chung T, Geva T. Phase-velocity cine magnetic resonance imaging measurement of pulsatile blood flow in children and young adults: in vitro and in vivo validation. Pediatr Cardiol 2000;21:104–10.
18. Holland BJ, Printz BF, Lai WW. Baseline correction of phase-contrast images in congenital cardiovascular magnetic resonance. J Cardiovasc Magn Reson 2010;12:11.
19. Chernobelsky A, Shubayev O, Comeau CR, Wolf SD. Baseline correction of phase contrast images improves quantification of blood flow in the great vessels. J Cardiovasc Magn Reson 2007;9:681–5.
20. Bernstein MA, Zhou XJ, Polzin JA, et al. Concomitant gradient terms in phase contrast MR: analysis and correction. Magn Reson Med 1998;39:300–8.
21. Miller TA, Landes AB, Moran AM. Improved accuracy in flow mapping of congenital heart disease using stationary phantom technique. J Cardiovasc Magn Reson 2009;11:52.
22. Lin LI. A concordance correlation coefficient to evaluate reproducibility. Biometrics 1989;45:255–68.
23. Bland JM, Altman DG. Statistical methods for assessing agreement between two methods of clinical measurement. Lancet 1986;1:307–10.
24. Schuirmann DJ. A comparison of the two one-sided tests procedure and the power approach for assessing the equivalence of average bioavailability. J Pharmacokinet Biopharm 1987;15:657–80.
25. Kramer CM, Barkhauser J, Flamm SD, Kim RJ, Nagel E. Standardized cardiovascular magnetic resonance imaging (CMR) protocols, society for cardiovascular magnetic resonance: board of trustees task force on standardized protocols. J Cardiovasc Magn Reson 2008;10:35.
26. Pennell DJ, Udo PS, Higgins CB, et al. Clinical indications for cardiovascular magnetic resonance (CMR): consensus panel report. Eur Heart J 2004;25:1940–65.
27. Hundley WG, Bluemke DA, Finn JP, et al. ACCF/ACR/AHA/NASCI/SCMR 2010 expert consensus document on cardiovascular magnetic resonance: a report of the American College of Cardiology Foundation Task Force on Expert Documents. J Am Coll Cardiol 2010;55:2614–62.

Key Words: cardiac magnetic resonance ■ congenital heart disease ■ right ventricular volumes.